JOURNAL OF NEUROSURGERY:
Case Lessons

J Neurosurg Case Lessons 9(20): CASE25152, 2025
DOI: 10.3171/CASE25152

Calcifying pseudoneoplasm of the neuraxis progressing to G5/PDGFRA subgroup glioblastoma in a United States Army veteran with a history of head trauma and germline POT1 and EPHB2 mutations: illustrative case

Maria-Magdalena Georgescu, MD, PhD,[1] Adriana Olar, MD, MSc,[2] and William Daniel Zollinger Jr., MD[3]

[1]NeuroMarkers, Houston, Texas; [2]NOMIX Laboratories, Denver, Colorado; and [3]Northeast Louisiana Radiation Oncology, Monroe, Louisiana

BACKGROUND Trauma-associated glioblastoma has been previously described, albeit without molecular characterization.

OBSERVATIONS The authors show the integrated clinical/pathologic/molecular analysis of a glioblastoma developing 43 years after head trauma sustained by a United States veteran. An epileptogenic benign lesion developed at the trauma site, followed 34 years later by a calcified lesion diagnosed as calcifying pseudoneoplasm of the neuraxis (CAPNON) that recurred 9 years later as glioblastoma with heterotopic/metaplastic ossification. Genomic analysis showed novel germline mutations in the telomere maintenance factor *POT1* p.W184* and receptor tyrosine kinase (RTK) *EPHB2* p.W792*. The somatic alterations included second-hit *POT1* p.D163Y mutation, *CDKN2A/2B* homozygous loss, *DNMT3A* mutation and *PDGFRA* amplification, classifying this glioblastoma in the G5/PDGFRA molecular subgroup. Proliferation markers, *PDGFRA*, MAPK feedback inhibitors, and *EPHB1* showed high expression, whereas *EPHB3* and *EPHA7* showed the highest expression of all glioblastomas. Following gross-total resection, the patient received adjuvant radiotherapy and temozolomide and died 16.3 months later.

LESSONS This is the first report of CAPNON progression to glioblastoma and of molecularly characterized glioma occurring decades after head trauma. A multifactorial etiology including genetic predisposition and posttraumatic repair is hypothesized. The discussion presents possible roles of EPH RTKs in posttraumatic repair and CAPNON, and of POT1 and PDGFRα in subsequent progression to glioblastoma.

https://thejns.org/doi/abs/10.3171/CASE25152

KEYWORDS trauma; posttraumatic glioblastoma; CAPNON; heterotopic; metaplastic ossification; germline mutations; PDGFRA; POT1; EPHB2; EPHB7 receptor tyrosine kinases; case report

Glioblastoma is the most frequent and aggressive primary brain tumor in adults. Except for rare cases of genetic predisposition,[1] the causes for its occurrence are not known, and there are no preventive tests for early detection. IDH-wildtype glioblastoma, previously called "de novo" to differentiate it from IDH-mutant astrocytoma, generally shows symptoms a few weeks before its radiological detection as a rim-enhancing mass and diagnostic histological features of necrosis and/or microvascular proliferation.[2] Only a small number of cases show nonenhancing lesions without diagnostic histological criteria but with diagnostic molecular criteria for glioblastoma: the presence of either *EGFR* amplification, *TERT* promoter mutation, or chromosomes 7 gain and 10 loss (7+/10−);[2] these patients usually show better survival.[3]

Cases with long intervals of symptomatic progression to IDH-wildtype glioblastoma are not well documented. In particular, trauma-associated glioblastoma is underexplored, with only a few case reports without molecular data.[4–7] Moreover, only very recently, a large-scale epidemiological study reported an association between trauma in US veterans and brain tumor development.[8]

In this study, we show a rare case of trauma-associated benign epileptogenic focus in an US veteran, progressing over decades to calcifying pseudoneoplasm of the neuraxis (CAPNON) and later on, to glioblastoma with heterotopic ossification. Paired normal/glioblastoma DNA and RNA next-generation sequencing (NGS) detected germline mutations in the receptor tyrosine kinase (RTK) *EPHB2* and in the

ABBREVIATIONS CAPNON = calcifying pseudoneoplasm of the neuraxis; CNV = copy number variation; HGNE = high-grade neuroendocrine; MAPK = mitogen-activated protein kinase; NGS = next-generation sequencing; RTK = receptor tyrosine kinase; TMZ = temozolomide; VAF = variant allele fraction.

INCLUDE WHEN CITING Published May 19, 2025; DOI: 10.3171/CASE25152.
SUBMITTED March 3, 2025. **ACCEPTED** April 2, 2025.

telomere maintenance factor *POT1*, as well as somatic alterations in *PDGFRA*, *CDKN2A/2B*, *POT1*, and *DNMT3A*. This constellation of alterations classified this tumor in the G5/PDGFRA molecular subgroup.[9,10] Expression analysis showed differential expression of EPH family RTKs and robust mitogen-activated protein kinase (MAPK) pathway activation, with implications for posttraumatic scar formation, heterotopic/metaplastic ossification, and oncogenic transformation.

Illustrative Case

The clinical data for this study were collected in paper file records followed by digital file records over a 45-year period. The paper file records contained the initial CT reports and the initial biopsy report. The initial raw materials, such as histological blocks/slides from approximately 40 years ago, were not available for our direct review, as they were subject to medical laboratory archiving regulations and disposed of after the established archiving period. Moreover, the CT imaging technology has been introduced historically in US medical practice after the patient's initial traumatic event.

A White-Caucasian male US Armed Forces veteran had a history of left frontal head trauma after hitting his head on a rock at 23 years of age during army service, resulting in a grand mal seizure for which he was placed on continuous antiepileptic medication but not hospitalized (Fig. 1A). A decade later, at 33 years, CT showed a scar-like mass in the left frontal lobe. A biopsy was performed, yielding nonspecific benign pathology. At 57 years of age, the patient developed slurred speech, and CT showed a large calcified cystic lesion in the left frontal lobe at the site of the previous biopsy. Subsequent MRI revealed a nonenhancing, solid and cystic 5.6-cm × 4.4-cm × 2.5-cm mass, containing calcification and hemorrhage, with adjacent edema noted in the left frontal and parietal lobes, significantly effacing the body and frontal horn of the left lateral ventricle and resulting in mild left-to-right subfalcine herniation. He underwent a left frontoparietal craniotomy with nearly gross-total resection of this lesion further diagnosed as CAPNON, with only a small residual lesion left. The patient was seizure free for the subsequent 9 years. At the age of 66 years, he presented for speech difficulty with finding words and progressive right upper and lower extremity weakness and numbness lasting 2 months. CT showed left frontoparietal recurrence, with coarse calcification measuring 2 cm × 1.4 cm in the wall of a large cyst measuring 7 cm × 3 cm (Fig. 1B). MRI showed rim enhancement, peripheral vasogenic

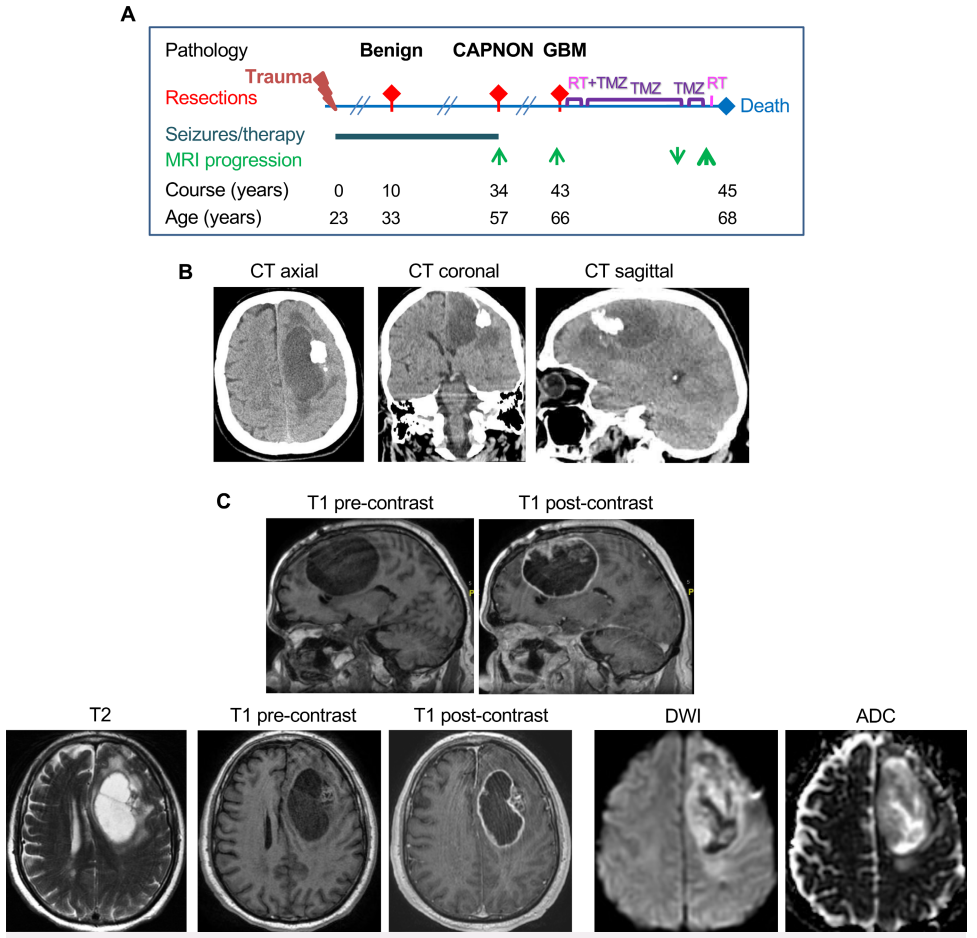

FIG. 1. Clinical presentation. **A:** Timeline showing evolution over 4 decades of a posttraumatic lesion to CAPNON and glioblastoma (GBM). *Red diamonds* indicate the initial biopsy and subsequent resections. **B:** Axial, coronal, and sagittal CT scans showing a left frontoparietal large cystic GBM with coarse anterolateral calcification. **C:** Sagittal (*upper*) and axial (*lower*) MR images showing rim enhancement of the cystic GBM, with several areas of restricted diffusion (compare the diffusion-weighted imaging [DWI] studies with the apparent diffusion coefficient [ADC] studies). RT = radiotherapy.

edema/infiltration, septations of the cyst, and restricted diffusion in several areas of the mass (Fig. 1C). Following functional MRI to outline the areas of speech and motor function that were not involved by the tumor, gross-total resection was performed, and the tumor was diagnosed as glioblastoma.

Standard adjuvant therapy consisting of concurrent temozolomide (TMZ) and radiotherapy to left frontoparietal brain (total dose 6120 cGy) for 7 weeks was started 1.5 months following tumor resection. TMZ was continued for 9 months, showing scar regression and no new masses at the end of this period. TMZ was not administered for 1.5 months due to a failure of the company to deliver it, and it was restarted when the drug became available. However, approximately 3 weeks after resuming TMZ, the patient became confused. MRI showed new areas of diffuse enhancement along the anterior corpus callosum crossing the midline (5.3 cm × 2.3 cm × 1.6 cm), right temporal lobe, anterior wall of the right lateral ventricle (0.7 cm in diameter), and additional rim-enhancing foci in the right frontal lobe (2.1 cm × 1.5 cm and 1.4 cm × 1.0 cm in the largest dimensions) and left cerebellar hemisphere (2.3 cm × 2.0 cm in the axial dimensions), consistent with glioblastoma recurrence. An additional solid malignancy was excluded by chest, abdominal, and pelvic CT. Palliative radiotherapy was delivered to the right frontal and cerebellar lesions (total dose 1000 cGy) and corpus callosum (total dose 720 cGy). The patient died less than 4 weeks after the end of the palliative radiotherapy (16.3 months after surgery).

Histological Analysis

The histological processing of the resected brain lesions was performed as previously described.[9,11] Formalin-fixed, paraffin-embedded sections of the resection specimens were stained with H&E, and processed for immunohistochemistry with GFAP (EP672Y), Olig-2 (387M-15), p53 (DO-7), Ki-67 (30-9) (Roche/Ventana Medical Systems Inc.), NeuN (MAB377, Chemicon/Millipore/Sigma), and IDH1-R132H (DIA-H09, Dianova).[12] The first mass, occurring at 57 years of age, showed the characteristics of CAPNON,[13] with a chondromyxoid, amorphous or calcified core bordered by palisading flattened or plump epithelioid cortical cells (Fig. 2A upper). Beneath the cortical cells, lumpy eosinophilic cords blended into a fibrous stroma that variably featured small, reactive, fibrillary cells and numerous Rosenthal fibers (Fig. 2A lower). Mitotic figures and foreign body reaction were absent. The edge and stromal cells were negative for GFAP, excluding pilocytic astrocytoma, an entity that can be in the differential diagnosis of CAPNON.[14] NeuN was also negative in the cells and highlighted the noninfiltrative nature of the lesion. Immunostains for IDH1-R132H, Olig2, p53, and Ki-67 were also negative throughout the lesion, indicating its nonproliferative nature.

The second mass, recurring at the age of 66 years (henceforth referred to as M66) at the same site, showed the characteristics of the previous CAPNON, except that beside calcifications, extensive superficial ectopic ossification was present, underlaid by chondromyxoid matrix, which was tightly apposed to gliotic cortex (Fig. 2B upper left; see also M66 glioblastoma with ectopic ossification at https://neuromarkers.org/database Histology). A sharp transition zone between the chondroid matrix and fibrous neuropil was noted, with numerous Rosenthal fibers (Fig. 2B upper center left). The palisading plump epithelioid cells and the stromal fibrillary cells continuing into the fibrous reactive neuropil were similarly present, only in significantly higher numbers that in the CAPNON (Fig. 2B). Mitotic figures were detected in the fibrillary cell population, indicating that this population of cells underwent neoplastic transformation. In addition, these latter cells appeared to secrete a myxoid matrix that further built the extracellular matrix of the full-blown hypercellular tumor adjacent to the CAPNON-like changes (Fig. 2B lower). The tumor featured microvascular proliferation (Fig. 2B green arrowheads) and necrosis, and was composed of intermediate-size, GFAP-positive infiltrating cells with round, oval or elongated irregular nuclei surrounded by haloes. This histology was consistent with glioblastoma with pre–high-grade neuroendocrine (HGNE) morphology, classified in the histological cluster 3/anaplastic cluster.[9,10] The tumor showed very high mitotic activity, with 7–9 mitotic figures/hpf, including atypical mitoses (Fig. 2B red arrowhead). Immunohistochemical results for IDH1-R132H and p53 were negative. The MGMT promoter methylation test was negative.

Molecular Findings

A comprehensive genomic and transcriptomic analysis was performed on the M66 glioblastoma sample. Paired normal and tumor DNA NGS with the xT 596-gene panel (Tempus Labs)[9,15] showed the presence of 2 germline pathogenic mutations, *POT1* p.W184* and *EPHB2* p.W792* (Fig. 3A) and of a variant of unknown significance in *TPMT* p.L69V, shown to decrease its enzymatic activity.[16] A second, somatic, likely pathogenic *POT1* p.D163Y mutation, at clonal variant allele fraction (VAF), most likely occurred on the second *POT1* allele (Fig. 3A). This mutation has been reported in several cases of non–small cell lung cancer (Cancer Hotspots, GDC, cBioPortal). Amplification of the *PDGFRA*, *KIT*, *KDR* locus on chromosomal arm 4q12 was accompanied by a pathogenic *PDGFRA* p.V536E mutation in the RTK transmembrane domain at subclonal VAF. Additional somatic alterations consisted of *CDKN2A/2B* homozygous loss, extending upstream to *MLLT3* gene. A somatic pathogenic mutation in the chromatin remodeling gene *DNMT3A* p.Y735C, occurring in M66 at clonal VAF, has been reported in 66 various tumors (Cancer Hotspots, cBioPortal) but also as a germline mutation with impaired enzymatic activity responsible for neurodevelopmental syndromes.[17] Overall, this mutation profile classified the M66 tumor in the G5/PDGFRA molecular subgroup, which represents the only glioblastoma subgroup where a significant number of cases lack *TERT* promoter mutations.[9,10,18]

Copy number variation (CNV) analysis using CytoSNP-850K version 1.1 BeadChip (Illumina)[11,15] showed a lack of chromosome 7+/10− and presence of 3 of the 5 most prevalent G5/PDGFRA subgroup CNVs,[10] loss of chromosomes 4q, 13, and 14 (Fig. 3B). Chromothripsis, a feature of aggressive tumors, occurred on chromosomes 9p, 13, and 17. This analysis also confirmed the NGS results for *PDGFRA/KIT/KDR* amplification and *CDKN2A/2B* homozygous loss.

RNA whole transcriptome analysis[9,12,19] showed very high *PDGFRA* expression for the M66 glioblastoma, in the 80th percentile of the G5/PDGFRA subgroup values, the latter being significantly higher than those from other glioblastoma subgroups (Fig. 3C).[9] In contrast, M66 *KIT* and *KDR* expression values were blunted, at the 47th and 60th percentiles, respectively. *KIT* and *KDR* genes show amplification in less than half of G5/PDGFRA subgroup tumors,[10] and even in amplified tumors, *KDR* expression values were not significantly elevated compared with other glioblastoma subgroups (Fig. 3C).[9]

We have previously shown that the expression levels of the MAPK feedback inhibitors DUSP4/5/6,[20] SPRY1/2/4,[21] and AKAP12[22] might quantitively reflect the activation of the MAPK by RTKs in glioblastoma,[19] A compound MAPK activation percentile, $P_{MAPK\ activation}$, was calculated for M66 relatively to the other 13 G5/PDGFRA subgroup tumors with expression data using Microsoft Excel (version 16.54, Microsoft Corp.) and the formula $P_{MAPK\ activation} = \left(\sum_{i=1}^{j} Pi\right) / j$, where i

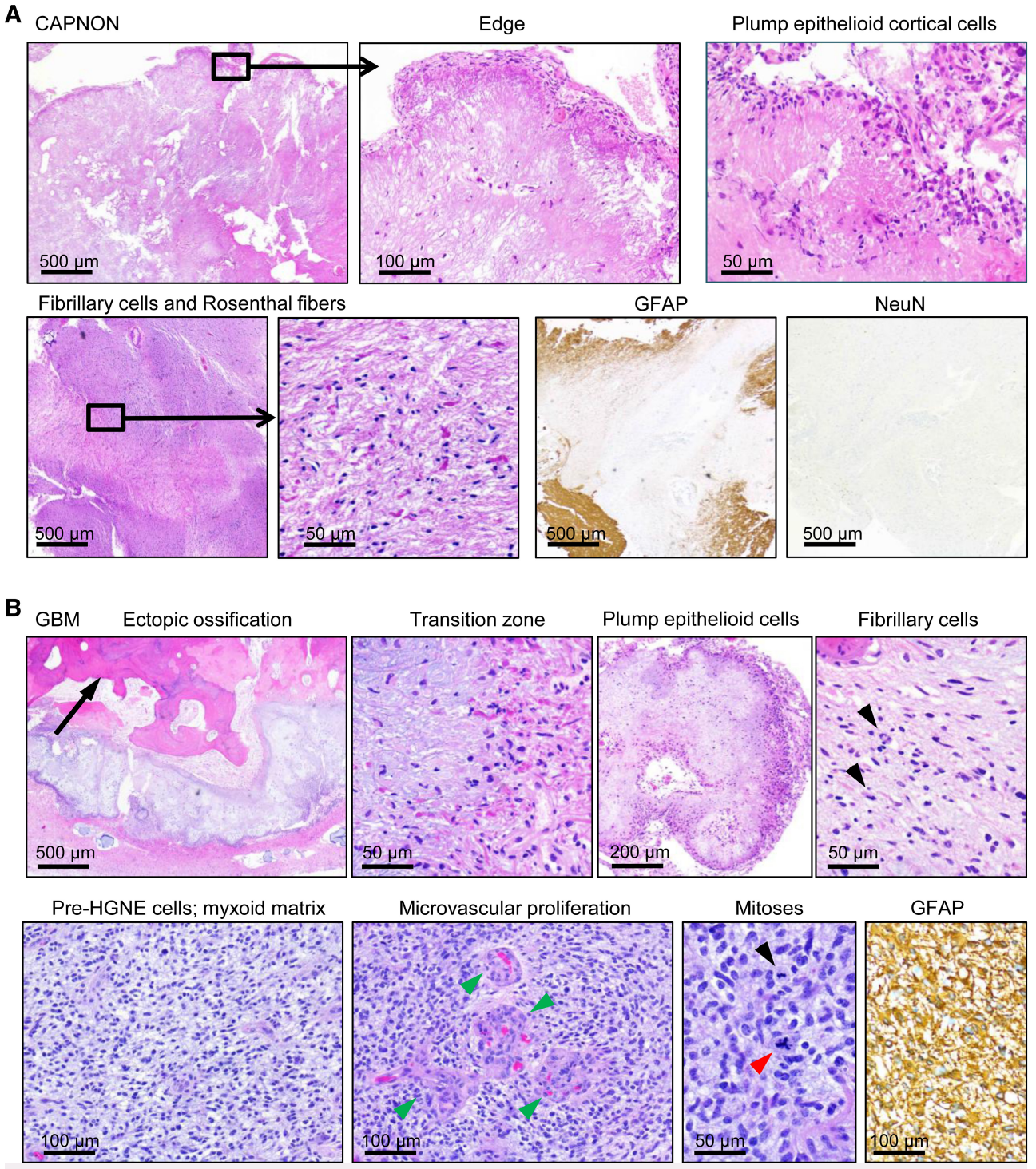

FIG. 2. Pathology. **A:** CAPNON H&E staining showing the calcified lesion bordered by a rim of flattened (**inset** magnified) or plump cortical cells (*upper*), and subjacent areas rich in Rosenthal fibers containing GFAP-negative and NeuN-negative small fibrillary cells (*lower*). **B:** Glioblastoma showing complex pathology, ranging from CAPNON-like areas with ectopic ossification (*arrow*), transition areas where mitotic figures (*arrowheads*) are noted in the fibrillary cell population (*upper*), and frank neoplastic areas (*lower*) with GFAP-positive pre-HGNE cells, microvascular proliferation (*green arrowheads*), and numerous mitotic figures. The *red arrowhead* indicates atypical mitosis.

represents an individual MAPK inhibitor of a total of $j = 7$ MAPK feedback inhibitors, and $Pi = k \times 100/n$ is its expression percentile, where k represents the ordinal rank and n, the number of ordered tumor expression values. The M66 MAPK activation was at 76th percentile in the G5/PDGFRA subgroup, suggesting strong MAPK activation in this tumor (Fig. 3D left).

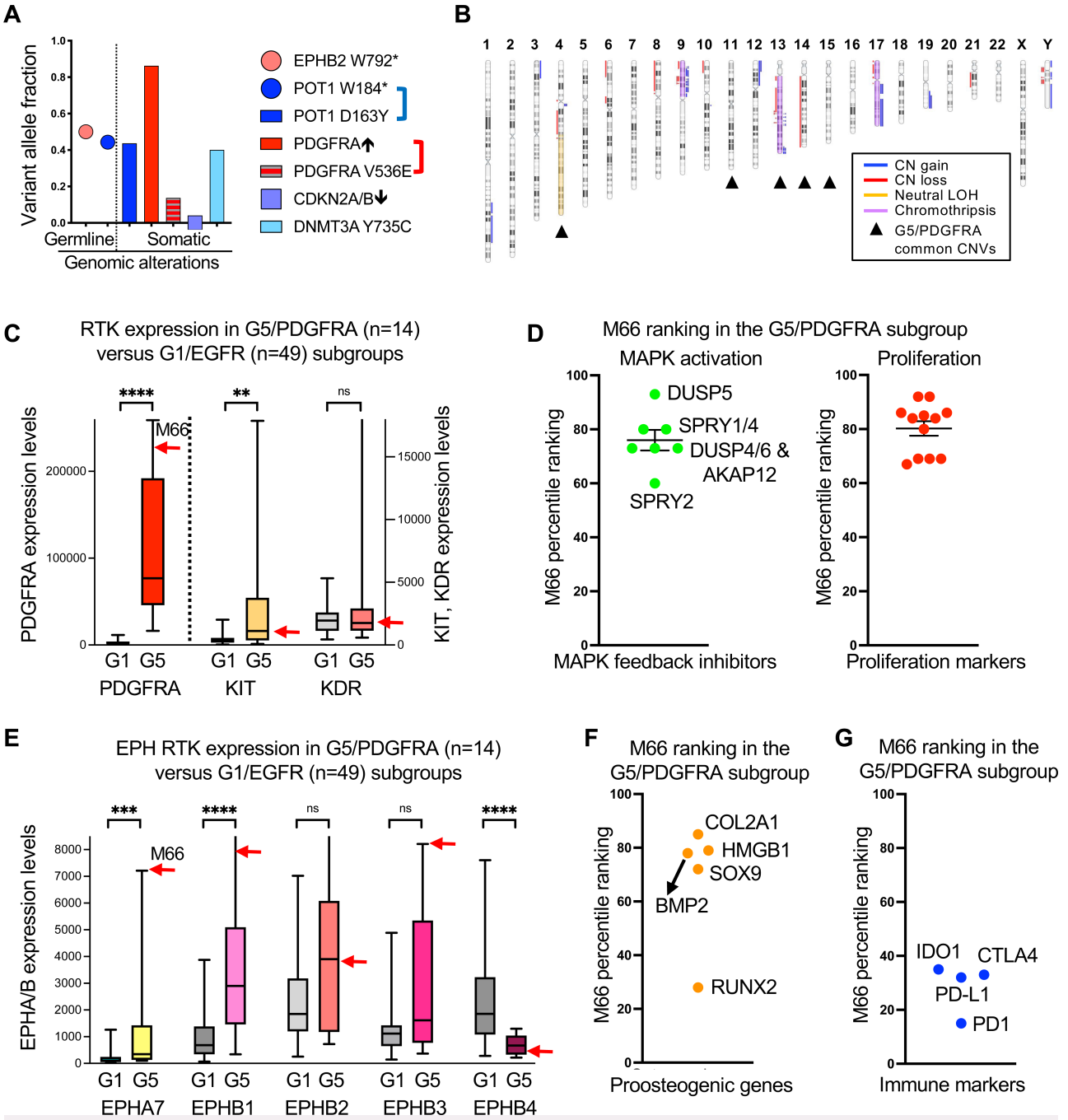

FIG. 3. Molecular assets of the M66 glioblastoma. **A:** Graph showing the VAF of germline and somatic alterations. **B:** Schematic karyotype representation showing CNVs. *Arrowheads* indicate 5 chromosomes commonly affected by whole arm/chromosome CNVs in G5/PDGFRA subgroup tumors compared with the other G1–G7 glioblastoma subgroups; note CNVs in 3 of these chromosomes in the M66 tumor. **C:** Boxplot expression analysis for chromosomal 4q12 locus RTKs (PDGFRA [left axis] and KIT, KDR [right axis]) in the G5/PDGFRA subgroup in comparison with the G1/EGFR subgroup tumors. The *box* represents the median and quartiles, and the *whiskers*, the minimum and maximum values. *Red arrows* indicate the expression value of the respective RTKs in the M66 tumor. Statistical significance was calculated using the Mann-Whitney nonparametric test. **D:** Dot plots showing M66 tumor percentile ranking in the G5/PDGFRA subgroup for MAPK activation (*left*) and proliferation (*right*), where each dot represents the percentile for a MAPK feedback inhibitor or proliferation marker, respectively. **E:** Boxplot expression analysis for indicated EPH RTKs, carried out as in panel C. **F and G:** Dot plots showing M66 tumor gene expression of pro-osteogenic genes (F) or immune checkpoint markers (G) as percentile ranking in the G5/PDGFRA subgroup. **p < 0.01; ***p < 0.001; ****p < 0.0001. LOH = loss of heterozygosity; ns = not significant; ↑ = gene amplification; ↓ = homozygous copy number.

The proliferation index percentile, $P_{proliferation}$, was calculated similarly, using the formula $P_{proliferation} = \left(\sum_{i=1}^{j} Pi\right) / j$, where *i* represents an individual proliferation marker of a total of *j* = 12 proliferation markers, and P*i* = *k* x 100/*n* represents its expression percentile, where *k* represents the ordinal rank and *n*, the number of ordered tumor expression values. These 12 proliferation markers (MKI67, TOP2A, TYMS, ODC, CCNB2, CDK1, CHEK1, BRCA1, BRCA2, BRIP1, FANCD2, and FANCI) were previously assessed for their accurate correlation with proliferation in glioblastoma.[9,19] The M66 glioblastoma proliferation index ranked in the 80th percentile of the G5/PDGFRA subgroup, in correlation with the very high mitotic index of this tumor (Fig. 3D right).

EPH RTK expression analysis showed very high expression for *EPHA7*, *EPHB1*, and *EPHB3* in the M66 tumor (Fig. 3E). In particular, the expression levels of *EPHA7* and *EPHB3* were the highest in the entire glioblastoma cohort (194 cases with RNA NGS).[10] In contrast, *EPHB2* and *EPHB4* leves were in the 47th and 33rd percentiles, respectively, of the G5/PDGFRA subgroup. In addition, *EPHA7* and *EPHB1* showed significantly higher expression values in the G5/PDGFRA subgroup compared with the G1/EGFR subgroup, in contrast to *EPHB4* (Fig. 3E). Other EPH RTKs showed nondistinct expression levels in the M66 tumor, either very low (*EPHA1*, *EPHA6*, *EPHA8*, *EPHA10*) or low (*EPHA2*, *EPHA3*, *EPHA5*, *EPHB6*). Similarly, other RTK expression levels were nondistinct, except for *MET* that showed undetectable levels in the M66 tumor.

The expression analysis of the Wnt/β-catenin, TGFβ/BMP, Hippo and Sonic Hedgehog (SHH) signaling pathways was performed as described previously[12] and showed lack of activation of these pathways. However, some of the pro-osteogenic genes, such as *COL2A1*, *BMP2*, *HMGB1*, and *SOX9*, showed relatively high values for M66, whereas *RUNX2* showed low values (Fig. 3F). The caveat of interpreting the contribution of these genes to ectopic bone formation is that transcriptomics was performed on the M66 tumor itself and not on the tissue closest to the bone. The immune markers CTLA4, PD1, PD-L1, and IDO1[23] showed collectively low expression in the M66 tumor (Fig. 3G).

Informed Consent

The necessary informed consent was obtained in this study.

Discussion

Observations

This study presents the evolution over decades of a trauma-associated epileptogenic lesion into CAPNON and subsequently to glioblastoma, 43 years after the traumatic event. The assumption that the head trauma preceded the epileptogenic focus and not vice versa in this case is based on the patient's history and on coinciding trauma location with ensuing pathologies. Several cases of posttraumatic glioblastoma have been reported, with similar long "incubation" periods spanning 5–35 years following trauma.[4–7] None of these reported posttraumatic glioblastoma cases were sequenced. Surprisingly, CAPNON has not been previously associated with preceding trauma, and only isolated CAPNON cases have been associated with co-occurring tumors such as ependymoma,[24] dysembryoplastic neuroepithelial tumor,[25] or IDH-wildtype low-grade glioma.[26] To add to the complexity of the current case, the M66 glioblastoma showed heterotopic/metaplastic ossification, an exceedingly rare occurrence in glioblastoma, mentioned in only 2 reports predating tumor sequencing.[27,28]

Figure 4 proposes a speculative mechanistic model in which the two germline mutations cooperated with the tissue repair and inflammatory response triggered by 2 external traumatic events, the initial

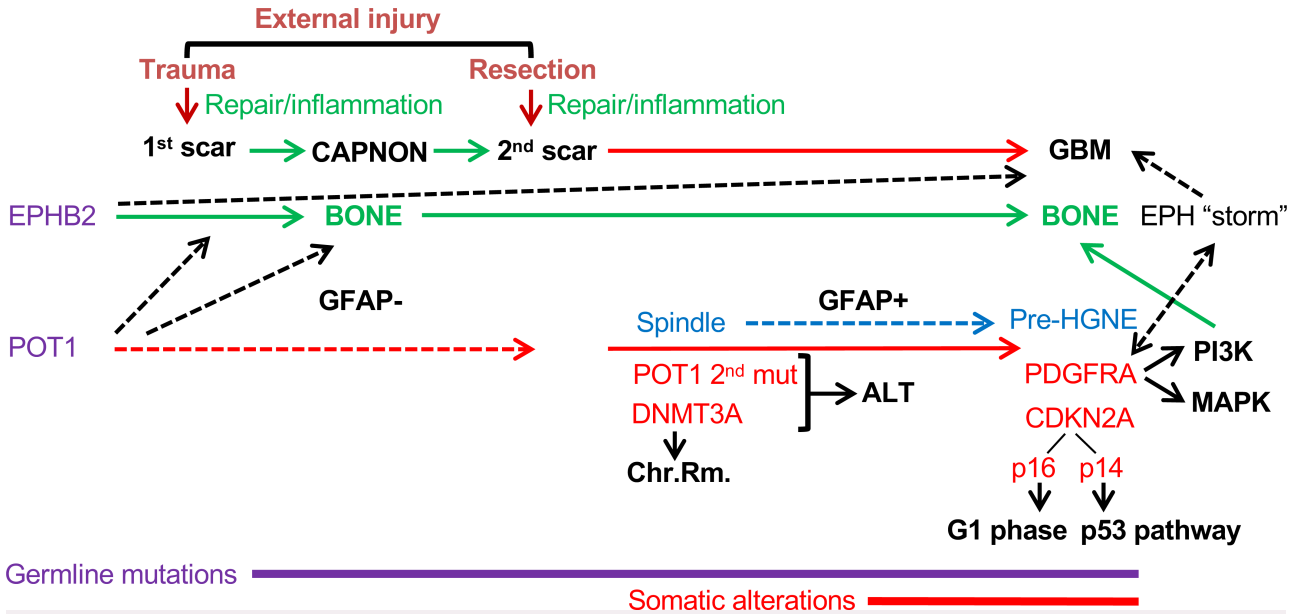

FIG. 4. Speculative mechanistic model of trauma-associated repair and evolution to CAPNON and glioblastoma in M66. Germline mutations (*purple*) contribute to both CAPNON with ectopic bone formation and GBM, with *solid* and *dotted arrows* indicating direct and more protracted causative effects, respectively. The GFAP expression is indicated, and histological changes are shown in *blue.* The somatic alterations are shown in *red*, and the growth pathways activated in the M66 tumor are indicated in *black*. ALT = alternative lengthening of telomeres; Chr.Rm. = chromatin remodeling; Mut = mutation.

trauma and the CAPNON subtotal resection 34 years later. In M66, the CAPNON fibrillary component was GFAP-negative, excluding an associated glioma at that time. The glioblastoma resection showed a complex histology, with 2 GFAP-positive morphologic components, a fibrillary one, close to the CAPNON-like changes, and a pre-HGNE one, with necrosis and microvascular proliferation that underwent molecular characterization.

An *EPHB2* germline mutation was detected by paired normal/tumor DNA NGS. Eph receptors form the largest class of RTKs, comprising 14 distinct members, classified as EphAs and EphBs.[29] Their major roles in physiological processes include angiogenesis, chondrogenesis and bone development and repair.[30] Together, EphB2, EphB1, EphB4 and EphA7 regulate the maintenance of the bone marrow stromal stem cell and hematopoietic stem/progenitor cell niche.[30] Although speculative, it is conceivable that postinjury, deregulation of Eph signaling and contribution from other proosteogenic factors, including the PI3K pathway,[31] led to abnormal wound repair, CAPNON, and heterotopic/metaplastic ossification (Fig. 4).

The somatic *PDGFRA* amplification classified the M66 glioblastoma in the G5/PDGFRA molecular subgroup that shows a high percentage of tumors with the similar characteristics, such as lack of genomic alterations in *TERT* promoter and PI3K pathway, and lack of chromosome 7+/10−.[9,10] Additionally, several chromosomal CNVs enriched in the G5/PDGFRA subgroup[10] were present in the M66 tumor. Of the 5 major pathways activated by genomic alterations in glioblastoma (RTK/MAPK, PI3K, telomere elongation, cell cycle G1 phase and p53 pathways),[9,10] the M66 glioblastoma showed oncogenic alterations in *PDGFRA* RTK, *POT1* telomere maintenance factor, and *CDKN2A* gene that simultaneously encodes p16/INK4A and p14ARF tumor suppressors involved in the cell cycle G1 phase and p53 pathways, respectively (Fig. 4).

PDGFRA amplification was accompanied by *KIT* and *KDR* RTK amplifications, with only *PDGFRA* amplification translated into very high overexpression. A *PDGFRA* p.V536E transmembrane domain mutation shown to stimulate ERK/MAPK activation in the absence of ligand and respond to imatinib inhibition[32] was also detected. Consequently, the ERK/MAPK and PI3K pathway feedback inhibitors were strongly upregulated in the M66 tumor, suggestive of both MAPK and PI3K pathway activation downstream of PDGFRα activation. The reason why PI3K pathway alterations, especially *PTEN* mutations, show significantly less incidence in the G5/PDGFRA subgroup[10] is not clear. In contrast to other RTKs, PDGFRα, and PDGFRβ recruit PTEN in complex with NHERF1 to attenuate the PI3K signaling,[33] and this direct mechanism of modulating PTEN activity might be sufficient to fine tune the PI3K signaling downstream PDGFRs.

Similar to other G5/PDGFRA cases or the G3/MMR cases,[23] *TERT* promoter mutations and *TERT* overexpression were absent in the M66 glioblastoma, indicating that an alternative lengthening of telomeres mechanism[34] is present in this case. Novel *POT1* germline p.W184* and somatic p.D163Y mutations mapping to the DNA-binding OB2 (oligonucleotide/oligosaccharide binding) fold domain were detected. POT1 is an essential subunit of the shelterin telomere binding complex that prevents the chromosome ends from shortening during DNA replication.[35] Its mutation results in dysregulation of telomere length and genomic instability, likely explaining the extensive chromothripsis from the M66 tumor. *POT1* germline mutations predispose to a variety of cancers, predominantly angiosarcoma, and very rarely glioblastoma.[36] Moreover, a second-hit somatic *POT1* mutation in glioblastoma appears to be a very rare event.[36] Therefore, it is reasonable to conclude that the *POT1* germline mutation predisposed this patient for glioblastoma development and that the second hit somatic mutation at clonal VAF was acquired early in the evolution of the tumor, perhaps initially in the fibrillary cell component (Fig. 4). An additional pathogenic mutation in the chromatin remodeling gene *DNMT3A* at clonal VAF was also detected. Although mutations in various chromatin remodeling genes occur in approximately 23% of glioblastomas,[10] a role for DNMT3A in telomere elongation and recombination has been demonstrated in genetically deficient cells that show dramatically elongated telomeres,[37] suggesting a possible compensation between mutant POT1 and DNMT3A in telomere elongation.

The role of EphB2 in glioblastoma neurospheres has been described as dichotomic, with silencing/loss-of-function, as in M66, stimulating proliferation and inhibiting migration.[38] In general, not only there is great complexity in Eph signaling, but the studies reporting Eph effects on cancer cells are focused on one Eph RTK at a time that may have opposing roles in different cancer types.[29,39] In the M66 glioblastoma, the *EPHB2* p.W792* germline mutation was accompanied by a "storm" of *EPHB1*, *EPHB3*, and *EPHA7* overexpression (Fig. 4). In addition, these Eph RTK expression levels appeared to be dependent on the G1–G7 glioblastoma subgroup, with significant differences between the G1/EGFR and G5/PDGFRA subgroups. Faced with this compounded complexity, it is difficult to evaluate the cumulative effect of Eph RTK expression changes on the M66 glioblastoma and their interrelationship with PDGFR RTKs.

Lessons

This is the first molecularly documented case of trauma-associated glioblastoma, and it shows an evolution through a wound repair process, including CAPNON development, most likely determined by germline mutations in *EPHB2* and *POT1*. The evolution of the pathology at the same site of the initial epileptogenic trauma and the presence of added somatic mutations onto a predisposing genetic background suggests a multifactorial etiology. The process of heterotopic/metaplastic ossification is extremely rare in glioblastoma but it is more common in CAPNON, so a grasp of this process could be obtained by paired normal/CAPNON sequencing and expression analysis. Since head trauma is relatively common in certain professions, including the army, the findings presented in this study set the foundation for understanding the basis of trauma-associated brain tumor development and personalized therapy.

Acknowledgments

Funding for this study was provided by NeuroMarkers.

References

1. Melin BS, Barnholtz-Sloan JS, Wrensch MR, et al. Genome-wide association study of glioma subtypes identifies specific differences in genetic susceptibility to glioblastoma and non-glioblastoma tumors. *Nat Genet*. 2017;49(5):789-794.
2. WHO Classification of Tumours. *Central Nervous System Tumours*. Vol 6, 5th ed. IARC Publications; 2021.
3. Lee M, Karschnia P, Park YW, et al. Comparative analysis of molecular and histological glioblastomas: insights into prognostic variance. *J Neurooncol*. 2024;169(3):531-541.
4. Anselmi E, Vallisa D, Bertè R, Vanzo C, Cavanna L. Post-traumatic glioma: report of two cases. *Tumori*. 2006;92(2):175-177.
5. Coskun S, Coskun A, Gursan N, Aydin MD. Post-traumatic glioblastoma multiforme: a case report. *Eurasian J Med*. 2011;43(1):50-53.

6. Moorthy RK, Rajshekhar V. Development of glioblastoma multiforme following traumatic cerebral contusion: case report and review of literature. *Surg Neurol*. 2004;61(2):180-184.
7. Zhou B, Liu W. Post-traumatic glioma: report of one case and review of the literature. *Int J Med Sci*. 2010;7(5):248-250.
8. Stewart IJ, Howard JT, Poltavskiy E, et al. Traumatic brain injury and subsequent risk of brain cancer in US veterans of the Iraq and Afghanistan wars. *JAMA Netw Open*. 2024;7(2):e2354588.
9. Georgescu MM. Multi-platform classification of IDH-wild-type glioblastoma based on ERK/MAPK pathway: diagnostic, prognostic and therapeutic implications. *Cancers (Basel)*. 2021;13(18):4532.
10. Georgescu MM. Translation into clinical practice of the G1-G7 molecular subgroup classification of glioblastoma: comprehensive demographic and molecular pathway profiling. *Cancers (Basel)*. 2024; 16(2):361.
11. Georgescu MM, Li Y, Islam MZ, et al. Mutations of the MAPK/TSC/mTOR pathway characterize periventricular glioblastoma with epithelioid SEGA-like morphology-morphological and therapeutic implications. *Oncotarget*. 2019;10(40):4038-4052.
12. Georgescu MM, Whipple SG, Notarianni CM. Novel neoplasms associated with syndromic pediatric medulloblastoma: integrated pathway delineation for personalized therapy. *Cell Commun Signal*. 2022;20(1):123.
13. Yang K, Reddy K, Chebib I, Hammond R, Lu JQ. Calcifying pseudoneoplasm of the neuraxis: from pathogenesis to diagnostic and therapeutic considerations. *World Neurosurg*. 2021;148:165-176.
14. Hernández-Reséndiz R, Villanueva-Castro E, Mateo-Nouel EJ, et al. Calcified pilocytic astrocytomas and calcifying pseudoneoplasms of the neuraxis: a diagnostic challenge. *Cureus*. 2024; 16(1):e51765.
15. Georgescu MM, Olar A. Genetic and histologic spatiotemporal evolution of recurrent, multifocal, multicentric and metastatic glioblastoma. *Acta Neuropathol Commun*. 2020;8(1):10.
16. Garat A, Cauffiez C, Renault N, et al. Characterisation of novel defective thiopurine S-methyltransferase allelic variants. *Biochem Pharmacol*. 2008;76(3):404-415.
17. Christian DL, Wu DY, Martin JR, et al. DNMT3A haploinsufficiency results in behavioral deficits and global epigenomic dysregulation shared across neurodevelopmental disorders. *Cell Rep*. 2020; 33(8):108416.
18. Higa N, Akahane T, Yokoyama S, et al. A tailored next-generation sequencing panel identified distinct subtypes of wildtype IDH and TERT promoter glioblastomas. *Cancer Sci*. 2020;111(10): 3902-3911.
19. Georgescu MM, Islam MZ, Li Y, Traylor J, Nanda A. Novel targetable FGFR2 and FGFR3 alterations in glioblastoma associate with aggressive phenotype and distinct gene expression programs. *Acta Neuropathol Commun*. 2021;9(1):69.
20. Kidger AM, Keyse SM. The regulation of oncogenic Ras/ERK signalling by dual-specificity mitogen activated protein kinase phosphatases (MKPs). *Semin Cell Dev Biol*. 2016;50:125-132.
21. Ornitz DM, Itoh N. The fibroblast growth factor signaling pathway. *Wiley Interdiscip Rev Dev Biol*. 2015;4(3):215-266.
22. Lin X, Nelson P, Gelman IH. SSeCKS, a major protein kinase C substrate with tumor suppressor activity, regulates $G_1 \rightarrow S$ progression by controlling the expression and cellular compartmentalization of cyclin D. *Mol Cell Biol*. 2000;20(19):7259-7272.
23. Georgescu MM. Adult glioblastoma with Lynch syndrome-associated mismatch repair deficiency forms a distinct high-risk molecular subgroup. *Free Neuropathol*. 2024;5:32.
24. Rodriguez FJ, Scheithauer BW, Fourney DR, Robinson CA. Ependymoma and intraparenchymal calcifying pseudoneoplasm of the neural axis: incidental collision or unique reactive phenomenon? *Acta Neuropathol*. 2008;115(3):363-366.
25. Yan X, Marsh WR, Scheithauer BW. Dysembryoplastic neuroepithelial tumor and calcifying pseudoneoplasms of the neuraxis: a collision of two seizure-associated lesions. *Clin Neuropathol*. 2011; 30(4):197-202.
26. Higa N, Yokoo H, Hirano H, et al. Calcifying pseudoneoplasm of the neuraxis in direct continuity with a low-grade glioma: a case report and review of the literature. *Neuropathology*. 2017;37(5): 446-451.
27. Nakamura O, Yamamoto H, Teramoto A, Takakura K, Nagashima K. Glioblastoma and fibrosarcoma in the brain with metaplastic bone formation—a case report. Article in Japanese. *No To Shinkei*. 1983;35(12):1185-1190.
28. Silbergeld DL, Wilkins P, Harkness WF, Bell BA. Subdural bone in a patient with glioblastoma multiforme. *Br J Neurosurg*. 1990;4(4): 349-352.
29. Guo X, Yang Y, Tang J, Xiang J. Ephs in cancer progression: complexity and context-dependent nature in signaling, angiogenesis and immunity. *Cell Commun Signal*. 2024;22(1):299.
30. Arthur A, Gronthos S. Eph-Ephrin signaling mediates cross-talk within the bone microenvironment. *Front Cell Dev Biol*. 2021; 9:598612.
31. Liu F, Zhao Y, Pei Y, Lian F, Lin H. Role of the NF-kB signalling pathway in heterotopic ossification: biological and therapeutic significance. *Cell Commun Signal*. 2024;22(1):159.
32. Velghe AI, Van Cauwenberghe S, Polyansky AA, et al. PDGFRA alterations in cancer: characterization of a gain-of-function V536E transmembrane mutant as well as loss-of-function and passenger mutations. *Oncogene*. 2014;33(20):2568-2576.
33. Takahashi Y, Morales FC, Kreimann EL, Georgescu MM. PTEN tumor suppressor associates with NHERF proteins to attenuate PDGF receptor signaling. *EMBO J*. 2006;25(4):910-920.
34. Zhao S, Wang F, Liu L. Alternative lengthening of telomeres (ALT) in tumors and pluripotent stem cells. *Genes (Basel)*. 2019;10(12): 1030.
35. Wu Y, Poulos RC, Reddel RR. Role of POT1 in Human Cancer. *Cancers (Basel)*. 2020;12(10):2739.
36. Shen E, Xiu J, Lopez GY, et al. POT1 mutation spectrum in tumour types commonly diagnosed among POT1-associated hereditary cancer syndrome families. *J Med Genet*. 2020;57(10):664-670.
37. Gonzalo S, Jaco I, Fraga MF, et al. DNA methyltransferases control telomere length and telomere recombination in mammalian cells. *Nat Cell Biol*. 2006;8(4):416-424.
38. Wang SD, Rath P, Lal B, et al. EphB2 receptor controls proliferation/migration dichotomy of glioblastoma by interacting with focal adhesion kinase. *Oncogene*. 2012;31(50):5132-5143.
39. Pasquale EB. Eph receptors and ephrins in cancer progression. *Nat Rev Cancer*. 2024;24(1):5-27.

Disclosures

The authors report no conflict of interest concerning the materials or methods used in this study or the findings specified in this paper.

Author Contributions

Conception and design: Georgescu. Acquisition of data: all authors. Analysis and interpretation of data: all authors. Drafting the article: Georgescu. Critically revising the article: Georgescu, Olar. Reviewed submitted version of manuscript: Georgescu, Olar. Approved the final version of the manuscript on behalf of all authors: Georgescu. Statistical analysis: Georgescu. Administrative/technical/material support: Georgescu. Study supervision: Georgescu.

Correspondence

Maria-Magdalena Georgescu: NeuroMarkers, Houston, TX. mmgeorgescu@yahoo.com.